

Toward Scalable Co-located Practical Learning: Assisting with Computer Vision and Multimodal Analytics^{*}

Xinyu Li^a, Linxuan Zhao^a, Roberto Martinez-Maldonado^a, Dragan Gašević^a and Lixiang Yan^{b,a}

^aCentre for Learning Analytics at Monash, Monash University, Melbourne, Australia

^bSchool of Education, Tsinghua University, Beijing, China

ARTICLE INFO

Keywords:

Multimodal Learning Analytics
Practical Learning
Computer Vision
Assist Learning Process

ABSTRACT

This study examined whether a single ceiling-mounted camera could be used to capture fine-grained learning behaviours in co-located practical learning. In undergraduate nursing simulations, teachers first identified seven observable behaviour categories, which were then used to train a YOLOv11-based detector. Video data were collected from 52 sessions, and analyses focused on Scenario A because it produced greater behavioural variation than Scenario B. Annotation reliability was high (F1=0.933). On the held-out test set, the model achieved a precision of 0.789, a recall of 0.784, and an mAP@0.5 of 0.827. When only behaviour frequencies were compared, no robust differences were found between high- and low-performing groups. However, when behaviour labels were analysed together with spatial context, clear differences emerged in both task and collaboration performance. Higher-performing teams showed more patient interaction in the primary work area, whereas lower-performing teams showed more phone-related activity and more activity in secondary areas. These findings suggest that behavioural data are more informative when interpreted together with where they occur. Overall, the study shows that a single-camera computer vision approach can support the analysis of teamwork and task engagement in face-to-face practical learning without relying on wearable sensors.

1. Introduction

Online education has expanded at breathtaking speed (Akpen et al., 2024). Massive open online courses (MOOCs), learning-management systems, and video-conferencing tools now allow millions to study “anytime, anywhere,” while every mouse click and keystroke is automatically logged (Kohnke et al., 2022; Li et al., 2025b). These digital traces have fuelled a flourishing learning-analytics ecosystem that helps instructors diagnose misconceptions, personalise feedback, and refine course design (Paulsen and Lindsay, 2024). Yet not every learning experience fits through a browser window. Laboratory experiments (Papalazarou et al., 2024), nursing simulations (Alsharari et al., 2025), maker projects (Hsu et al., 2017), and design studios (Rosa and Ferreira, 2023) depend on physical artefacts, shared spatial layouts, and subtle face-to-face coordination. For such activities, a purely virtual substitute—or even an expensive AR/VR replica—still falls short pedagogically and financially (Li and Liang, 2024; Alsharari et al., 2025; Burke et al., 2025).

In colocated classrooms, socio-spatial behaviour therefore becomes a crucial source of evidence (Riquelme et al., 2020). Where the teacher stands, which peer group a student joins, how long collaborators remain shoulder-to-shoulder, and whether learners are typing, writing, or manipulating equipment all signal engagement, role taking, and emerging group dynamics (Fernandez-Nieto et al., 2021). Decades of classroom research corroborate these connections: teacher roaming patterns co-vary with instructional focus, students’ trajectories predict collaboration quality, and overall motion relates to learning outcomes (Lim et al., 2012; Yan et al., 2022a). Unfortunately, collecting such evidence at scale is far harder in a physical classroom than in an online platform.

Multimodal learning analytics (MMLA) offers two main strategies for bridging this gap. The first equips every participant with indoor-positioning tags such as ultra-wideband or Bluetooth beacons (Ochoa, 2022; Martinez-Maldonado et al., 2018; Nguyen et al., 2020). Tag data can be strikingly precise, enabling proximity graphs, heat maps, and teacher circulation metrics (Saqib et al., 2018; Martinez-Maldonado et al., 2020). But large deployments

✉ xinyu.li1@monash.edu (X. Li); linxuan.zhao@monash.edu (L. Zhao); roberto.martinezmaldonado@monash.edu (R. Martinez-Maldonado); dragan.gasevic@monash.edu (D. Gašević); lixiang.yan@monash.edu (L. Yan)

ORCID(s): 0000-0003-2681-4451 (X. Li); 0000-0001-5564-0185 (L. Zhao); 0000-0002-8375-1816 (R. Martinez-Maldonado); 0000-0001-9265-1908 (D. Gašević); 0000-0003-3818-045X (L. Yan)

are costly, logistically taxing, and disruptive: dozens of devices must be purchased, charged, and calibrated, and anchors must be installed throughout the room (Yan et al., 2022b; Saquib et al., 2018).

A second strategy relies on computer vision. An inexpensive ceiling camera combined with deep-learning detectors can track dozens of people in real time at a fraction of the cost of tags (Ahuja et al., 2019). However, most vision systems still answer only the “where”: who is close to whom and how they move (Li et al., 2023). They seldom recognise the “what.” Whether a student near a desk is reading notes, scrolling a phone, or programming a robot is pedagogically decisive yet invisible in today’s spatial heat maps.

This semantic gap contrasts sharply with online learning analytics, where low-level clicks are routinely converted into high-level constructs such as cognitive engagement or help-seeking (Li et al., 2025c; Chen et al., 2025). Achieving similar richness in colocated classrooms requires a method that can (1) detect the fine-grained actions learners perform, (2) situate those actions in space and time, and (3) demand no wearable sensors or specialist installation. Building such a method is the focus of the present work.

We propose a lightweight computer-vision pipeline that integrates socio-spatial tracking and action recognition from a single video stream. Leveraging the latest YOLOv11 object-detection architecture (Khanam and Hussain, 2024), our system simultaneously outputs each participant’s position and a label describing what they are doing—typing on a laptop, using a phone, writing on paper, manipulating domain-specific equipment, or observing peers. Because YOLOv11 is optimised for speed, hours of classroom footage can be processed on a commodity GPU within minutes, opening a path toward real-time feedback. Crucially, the hardware requirements are minimal: one ceiling-mounted camera and a brief homography calibration suffice; no tags, beacons, or frequent recalibrations are needed even when furniture is rearranged.

Fusing “where” and “what” yields three concrete benefits. First, the approach preserves the low cost and non-intrusiveness of vision-based analytics, enabling large-scale or long-term deployment without burdening teachers or students. Second, the added semantic layer allows more actionable indicators. Two learners seated side by side may appear equally engaged in a trajectory map, but if one is texting and the other is coding collaboratively, the instructional response should differ. Third, the resulting traces generalise across domains: the same pipeline can illuminate participation equity in a project-based engineering course, teacher–student prompting patterns in a language lesson, or tool-handling sequences in a nursing simulation.

In summary, our contributions are: (1) a novel and generalizable methodology for capturing fine-grained socio-spatial data and learning actions in physical classroom settings via an AI-driven computer vision pipeline; and (2) empirical demonstrations of how these automatically captured traces can yield new insights into collaborative learning – for example, by visualizing group participation patterns, mapping teacher–student interaction networks, and comparing engagement across different pedagogical designs. We envision that this approach can be utilised across domains to help researchers and educators better understand the nuanced interplay of space, social interaction, and learning, ultimately supporting more reflective and effective colocated collaborative learning experiences.

2. Background

2.1. Online Versus In-Person Learning Analytics

Modern online courses operate inside software platforms that are instrumented by design (Torre et al., 2020). Every click on a button, every keystroke in a discussion forum, and every millisecond of video playback is logged automatically by the same servers that deliver content to the learner (Torre et al., 2020). Because these events are already formatted, time-stamped, and aligned with the curriculum, they can be transformed almost immediately into high-level constructs such as self-regulation (Li et al., 2025a), or help-seeking (Chen et al., 2025). A tutor dashboard that highlights which students re-watched a difficult explanation or which quiz items continue to cause confusion therefore costs little more than a database query (Paulsen and Lindsay, 2024). Researchers have exploited this abundance by training predictive models that flag at-risk learners, recommend targeted resources, or even adapt sequencing in real time (Ramaswami et al., 2023). The key enabler is the tight coupling between behaviour and instrumentation: the very device on which learning happens is the device that records the data.

The same coupling is conspicuously absent in face-to-face settings (Martinez-Maldonado et al., 2023). Physical artefacts—workbenches, microscopes, soldering irons—possess no intrinsic logging capability, and learners often act in ways that leave no digital footprint (Zhang et al., 2024). A student may sketch a circuit on scrap paper, whisper advice to a peer, or manipulate a shared robot without touching a computer at all (Holm-Janás et al., 2024). Capturing such behaviour requires external sensors that must be bought, installed, and maintained, turning what is essentially a software

problem online into a hardware and logistics problem on campus (Martinez-Maldonado et al., 2023). Institutions also face constraints that software rarely encounters: classrooms are reconfigured each semester, devices get misplaced, and maintenance budgets fluctuate (Chua et al., 2024). As a result, in-person teaching environments remain what some scholars describe as “data deserts,” rich in human activity yet poor in machine-readable evidence (Blikstein, 2013). Without that evidence, the sophisticated analytics that have become routine online—early-warning systems, adaptive recommendations, rapid A/B experimentation—are exceedingly difficult to transplant to physical classrooms (Yang et al., 2020).

2.2. Multimodal Learning Analytics Approaches

Aware of this deficit, the multimodal learning analytics (MMLA) community has spent the last decade experimenting with sensor combinations that can restore at least part of the lost observability (Ochoa et al., 2017). Indoor-positioning systems have been a prominent starting point. By asking every participant to wear an ultra-wideband, Bluetooth, or RFID tag, researchers can triangulate positions at sub-metre accuracy and reconstruct trajectories that reveal who gathered around which table, how long teams stayed together, and how evenly an instructor circulated (Zhao et al., 2022). Empirical work has shown that equitable teacher movement correlates with perceptions of support and that cohesive proximity patterns within groups predict higher task performance (Feng et al., 2024). Nevertheless, the logistical costs are steep. Tags must be distributed at the start of each session, charged overnight, and recalibrated whenever the floor plan changes. Anchors fixed to ceilings or walls need stable power and network connections, and technical failure in any component compromises the entire dataset (Saquib et al., 2018; Ahuja et al., 2019; Chng et al., 2020; Mallavarapu et al., 2022).

To deepen the behavioural picture, many MMLA studies layer additional sensors on top of location tracking. Lapel microphones record speaking turns, depth cameras capture posture and gesture, and physiological bands measure arousal or stress (Echeverria et al., 2024). When these streams are synchronised, they yield nuanced insights; for example, balanced vocal participation combined with dense face-to-face proximity has been linked to superior problem-solving outcomes (Zhao et al., 2023b). Yet each added modality multiplies complexity. Audio must be diarised and possibly transcribed, physiological signals require baselining and de-noising, and cross-modal synchronisation must be maintained to the millisecond (Zhao et al., 2024a). Consequently, although such systems have proven theoretically illuminating, they remain fragile prototypes. They demand technical expertise for daily operation and are rarely adopted outside controlled research studies (Zhao et al., 2023a). These experiences reveal a persistent tension. Rich multimodal data clarify collaborative processes and instructional effectiveness, yet the hardware and labour required to gather them exceed the appetite of most educational institutions. What the field lacks is a sensing approach that produces data of comparable semantic depth at a fraction of the logistical burden (Ochoa, 2022; Martinez-Maldonado et al., 2018; Nguyen et al., 2020).

2.3. Advances in Computer Vision

Recent progress in computer vision offers a promising resolution to that tension. A single ceiling-mounted RGB camera can now function as a multi-purpose sensor, delivering both spatial and semantic information in real time (Bosch et al., 2018). Modern object detectors such as YOLOv11 (Khanam and Hussain, 2024) and DEIM (Huang et al., 2025), or transformer-based models like DETR (Zhao et al., 2024b) and RT-DETR (Lv et al., 2024), localise every person in a room at video frame rates on commodity hardware. Through a one-time homography calibration, the system projects bounding-box centroids onto the floor plane, producing positional accuracy that rivals Bluetooth beacons while eliminating the need for wearables (Li et al., 2023). Because the hardware consists mostly of an inexpensive camera and an existing computer or edge device, the upfront investment is modest and no per-student maintenance is required.

Crucially, the same video feed can now reveal what each learner is doing. The deep learning computer vision models can differentiate learners behaviours between typing on a laptop, writing on paper, manipulating lab apparatus, or using a phone (Sümer et al., 2021). When these labels are time-aligned with spatial proximal position, the resulting dataset transcends mere trajectories (Tsai et al., 2016). An instructor could examine a heat map coloured by activity type rather than simple occupancy, or receive a real-time notification when a group that had been programming collaboratively shifts to idle phone use (Alzoubi et al., 2021). Such semantically enriched analytics align closely with the everyday questions of teaching practice: Which teams are genuinely engaged? Who might need a prompt or a scaffold? Where is off-task behaviour clustering? The practical advantages extend beyond instructional relevance. Vision-only systems avoid the daily hassle of distributing, charging, and collecting wearable tags, relying instead on inexpensive fixed cameras while still providing positional accuracy (Tsai et al., 2016). On-device processing allows raw footage to

be discarded immediately after inference, with only anonymised coordinates and activity codes stored for analysis. Techniques like face blurring or full image redaction satisfy many institutional review boards, mitigating one of the chief objections to classroom cameras (Zhang et al., 2021; Li et al., 2023).

When viewed in sequence, the logic becomes clear. Online platforms demonstrate the power of abundant, finely grained behavioural data. Multimodal sensor suites replicate some of that power in physical classrooms but at prohibitive cost and complexity. Advances in computer vision now promise the same depth of insight through a single, low-cost, minimally intrusive device. By merging spatial tracking and action recognition in one pipeline, vision-based analytics can finally offer a practical, scalable way to turn the “data desert” of face-to-face learning into fertile ground for evidence-informed pedagogy.

3. Computer Vision for Learning Behaviours Detection

In this paper, we propose a scalable and practical computer-vision approach for recognising learning behaviours in video recordings of co-located collaborative classrooms. As summarised in Figure 1, the end-to-end pipeline unfolds in three interlocking phases, including Learning Context Infusion, Computer-Vision Model Creation and Computer-Vision Deployment. So that every technical decision remains anchored in pedagogical intent while meeting the twin requirements of reliability and privacy.

3.1. Learning Context Infusion

The first phase, Learning Context Infusion, invites teachers and researchers to determine which actions are pedagogically meaningful in a particular lesson design. In a nursing-simulation study, for instance, stakeholders agreed on seven focal behaviours: *Using Computer, Document/Note Interaction* (noted as *Doc/Note Interaction* in following text), *Using Phone, Medication/Equipment Interaction* (noted as *Medi/Equip Interaction* in following text), *Sitting, Patient Interaction* and a residual *Other* category. All but *Sitting* can occur at any moment during the session; the *Sitting* label is reserved for a teacher who impersonates a patient’s relative and tries to distract the students and this labelled data can be filtered in data analysis. Because the taxonomy is derived directly from domain experts, it can be adapted to any other educational context without researcher intervention and revised as learning designs evolve. Short video excerpts are repeatedly reviewed with the stakeholders until every label corresponds unambiguously to an observable cue in a well-defined spatial region, establishing a shared interpretive frame before large-scale annotation begins.

3.2. Computer Vision Model Creation

After the behaviour taxonomy is finalised, we create a training set that reliably links visual evidence to those categories. The process unfolds in four steps: data sampling, data annotation, reliability check, and model training.

- **Data Sampling.** Instead of annotating every video frame, we applied uniform temporal sampling to obtain a diverse but manageable subset of images. Beginning at the “handover” moment—when students start performing the simulation task—we extracted one frame every 10 s from each session. The interval preceding the handover was excluded because, during this period, students were only receiving instruction from the lead teacher and were not engaged in task-related actions. This procedure produced 6,192 candidate frames, from which we randomly selected 10 frames from each session for manual annotation.
- **Data Annotation.** Two trained annotators first labelled the same subset of the data to assess inter-rater reliability. After this calibration step, they split the remaining dataset in half and annotated their respective portions independently. Using Label Studio’s video-annotation tool (Tkachenko et al., 2020-2025), each annotator drew tight bounding boxes around every person and task-relevant object (e.g., computer, medical equipment, patient manikin) and assigned an action label from the agreed-upon taxonomy (e.g., “Using Computer”).
- **Reliability Check.** Inter-rater reliability is computed on the double-coded pool using frame-level Cohen’s k (for action labels) and mean Intersection-over-Union (mIoU) for box overlap. We predefined acceptance criteria of $k \geq 0.80$ and $mIoU \geq 0.70$ before merging the two raters’ annotations. After reviewing the few remaining disagreements in a third-pass meeting, the raters reached consensus.
- **Model training.** The labelled image set is divided by stratified random sampling into 70 % training, 20 % validation, and 10 % test splits, guaranteeing that every action class appears in all three subsets. Throughout

the annotation process we monitored class counts; whenever the ratio of the most frequent to the least frequent class exceeded 5 : 1, additional frames for the under-represented class were added, following the guideline of Buda et al. Buda et al. (2018). Training starts from the public YOLOv11 “x-large” weights pre-trained on COCO. The network is fine-tuned for 60 epochs on an NVIDIA RTX 4090 GPU (24 GB VRAM) with a batch size of 16, yielding a throughput of ≈ 66 images per second and a total training time of about five minutes. The checkpoint with the highest mAP@0.5 on the validation set is retained for subsequent testing and analysis.

3.3. Computer Vision Deployment

After training, the model is deployed to identify learning behaviours in real time. The video stream first passes through an automated privacy module that detects and blurs all faces, ensuring anonymity for students and instructors. The de-identified frames are then fed to the fine-tuned YOLOv11 network, which can operate at webcam frame rates. For each frame, the model outputs time-stamped bounding boxes and action labels; these detections are both logged to disk and overlaid on the video via OpenCV (Bradski, 2000) for immediate visual feedback. The resulting behaviour log can be synchronised with additional data sources—such as indoor-positioning signals, seat maps, audio sentiment, or instructor annotations—to create rich socio-spatial analytics (e.g., heat maps of collaborative activity or temporal networks of peer interaction). An interactive dashboard lets educators filter events, replay critical moments, and export numerical summaries, thereby converting raw video into actionable insights while preserving learner privacy and maintaining methodological rigour

3.4. Research Questions

The following research questions were investigated to assess the reliability of the trained model and whether the learning behaviours recognised can reflect some educational insights. For the third research question, the prior study CVPE method is used together with the learning behaviours identification to further gain insights about how socio-spatial data and learning behaviours differ between high- and low-performing students.

- **RQ1:** To what extent can a computer-vision approach accurately detect students’ task-related behaviours in a complex, collaborative learning environment?
- **RQ2:** How do the task-related behaviours of nursing students differ between groups that achieve high versus low performance outcomes?
- **RQ3:** When the detected behaviours are combined with spatial position data (via CVPE), what additional insight do we gain into the differences between high- and low-performing groups?

4. Methods

4.1. Learning Context

The study was conducted in a compulsory third-year undergraduate nursing course that integrates high-fidelity clinical simulations. Across a four-week block, students worked in teams of four to participate the simulations. These simulations we conducted over 3 years and we choose the data from 2021 to 2022 because these two years’ data have similar classroom settings, such as the video recording camera position and the main task areas are similar. The simulations took place in a purpose-built classroom that replicated an acute ward environment. Each of the four beds was equipped with a high-fidelity manikin, wall oxygen, a vital-signs monitor, and other standard ward equipment (see Figure 2). Several events were pre-programmed—for example, a formal handover, the insidious or sudden deterioration of a patient, and telephone calls from family members, with students received no advance warning about which events would occur or which patient would deteriorate. This design created a fully immersive setting in which students could practise team communication, task prioritisation, and clinical decision-making under conditions that closely resembled actual practice.

Two distinct scenarios structured the simulation exercise. Scenario A featured a subtly deteriorating patient whose decline could be recognised only through a systematic assessment of vital signs, whereas Scenario B presented an overtly deteriorating patient and an accompanying family member (played by teaching staff) who actively sought help. For analytic purposes, the simulation room was partitioned into “spaces of interest,” hierarchically ordered according to instructional priority as outlined by teachers (Yan et al., 2022a). Figure 2 illustrates this spatial configuration. In both scenarios, Bed 4 (the deteriorating patient) and the adjacent phone used to activate a medical emergency team

Table 1

Teacher assessment items on students' team task and collaboration performance

| Item | Details |
|------|---|
| T1 | The students have demonstrated a structured approach to patient assessment and management. |
| T2 | The students have recognised and responded to early signs of patient deterioration. |
| T3 | The students have appropriately activated MET calls. |
| T4 | The students have contributed to effective teamwork. |
| T5 | The students have communicated information effectively to the health care team. |
| T6 | The students have demonstrated an understanding of the roles of the multidisciplinary team. |

(MET) constituted the primary task spaces. Behaviour occurring in these locations was deemed critical because it reflected students' ability to identify patient deterioration and initiate a MET call. Secondary task spaces included Beds 1 and 2 and the two intravenous stations. Although these areas were relevant during the initial patient handover, they should have received minimal attention once deterioration at Bed 4 became apparent. In Scenario A, Bed 3 served as a designated distraction space: a staff member, acting as a patient's relative, persistently diverted the team by requesting discharge procedures for her husband. Scenario B lacked this planned distraction, and therefore Bed 3 was categorised simply as a secondary task space.

Only data from Scenario A were analysed in the present study ($M = 20.8$ minutes, $SD = 5.3$ minutes). In Scenario B, all student teams rapidly converged at Bed 4, leading to less learning behaviours, such as "Computer Use" and "Medical/Equipment Interaction", which is difficult to support a meaningful analysis. Scenario A, by contrast, elicited a wider range of observable learning actions and interactions, allowing for a more robust examination of teamwork, task prioritisation, and response to distraction. Hence, we only choose Scenario A dataset for analysis in this paper.

4.2. Apparatus and Data Collection

All 52 simulation sessions were video-recorded with a Jabra 180-degree wide-angle webcam (approximately USD 600). The extreme field of view was required because the simulation ward is long and narrow; a single centrally mounted device had to capture every predefined "space of interest." Any camera that can record the full room would be adequate. After each session, the two facilitating academics completed a six-item formative assessment rubric aligned with the learning design (Table 1). Items T1–T3 evaluate task performance (e.g., timely identification of patient deterioration, correct activation of the MET call); Items T4–T6 evaluate collaborative behaviours (e.g., information sharing, leadership, mutual support). Each item is rated on a seven-point bipolar Likert scale (1 = *strongly disagree*, 7 = *strongly agree*). These teacher ratings serve as the criterion measure against which automated behavioural indicators are compared.

4.3. Ethics and Privacy Protection Measures

The ethics was obtained from the Monash University Human Research Ethics Committee (Project ID 28026). Participation was voluntary, and written informed consent was secured from all students and staff before recording. A session proceeded only when every member of the four-student team provided consent.

To protect privacy, all faces in the video were automatically obscured. During post-processing, each human bounding box detected by a YOLOv11 model was overlaid with an opaque rectangle with OpenCV covering the upper 20% of the box (see Figure 2). The same algorithm can be executed in real time should the recordings ever be streamed. All data are stored on an encrypted university server accessible only to the research team, and no unmasked footage is released outside that environment.

4.4. Learning Behaviours

As outlined in Section 3, we first trained a computer-vision model on an annotated image set that uses the full set of predefined learning behaviour categories (Table 2). The learning behaviours are identified by teachers. All data labelled as the code *Sitting* will be filtered in later data processing. Because this data point means the teacher is trying to distract students and its movement or learning actions have no relation to students' performance. Once trained, the model was able to classify the learning behaviour of students in each video frame.

To situate those behaviours within the pedagogical layout of the ward, we next overlaid geometric reference points on the classroom panorama. Several centroids were assigned to each space of interest: primary task areas (Bed 4 and

Table 2

Learning behaviours identified from video recordings.

| Code | Learning behaviours description |
|------------------------|---|
| Using Computer | The students stay near the computer and use the computer to check/record information. |
| Doc/Note Interaction | The students interact with document/note. |
| Using Phone | The students pick up phones and chatting in a phone call. |
| Medi/Equip Interaction | The students conduct operations with medication or medical equipments. |
| Sitting | The teachers played relative sitting on a seat. |
| Patient Interaction | The students interact with the patients such as chatting or conduct some checks. |
| Other | The students are moving, talking, or other unidentified behaviours. |

the MET telephone), secondary task areas (Beds 1–2 and the two intravenous stations), and the distraction space (Bed 3). Additional centroids were positioned in the corridors separating these zones to capture transitional movement.

For every frame we calculated the Euclidean distance between the midpoint of a student’s bounding box and each centroid. The space associated with the smallest distance was taken as that student’s location for the corresponding second. This procedure produced a time-stamped sequence that combines (a) the behaviour label generated by the vision model and (b) the socio-spatial context in which that behaviour occurred.

Integrating behavioural and spatial information allows us to extract pedagogically meaningful patterns that conventional computer-vision method cannot reveal. Earlier CVPE Li et al. (2023) work could only infer whether students were “working together” or “working individually.” Our enhanced pipeline, by contrast, differentiates fine-grained actions (e.g., *Using Computer*, *Medi/Equip Interaction*) and links them to critical task zones like primary and secondary areas (prim_ and sec_ prefixes will be used to indicate the learning actions happen in which area). Consequently, we can examine not simply whether students collaborate, but how their collaboration unfolds relative to task priorities and environmental distractions.

4.5. Model Reliability Analysis (RQ1)

To ensure that the performance gains observed during training were not the result of random chance or over-fitting, a comprehensive reliability analysis was carried out on the fine-tuned YOLOv11 model. The procedure began by splitting the annotated dataset into five, mutually exclusive folds so that k-fold cross-validation could be performed; this enabled the model to be trained and evaluated on different subsets of data, thereby providing a more robust estimate of its generalization capabilities. All the image data has been labelled by two experts of the nursing study with high inter rater reliability reached (see Table 4). Key reliability metrics—including mean Average Precision (mAP), precision, recall, and the F1-score—were computed for each fold, and their variances were examined to detect any instability across runs. In addition, confusion matrices were aggregated to highlight systematic misclassifications, while confidence-score distributions were inspected to verify that the model’s probability outputs were well-calibrated. Finally, statistical significance tests, such as paired t-tests against a baseline detector and bootstrapped confidence intervals around the mAP values, were employed to validate that the observed improvements were not merely incidental. The outcome of this multi-faceted analysis confirmed that the fine-tuned YOLOv11 model consistently delivered reliable object-detection performance across diverse data splits and operating conditions.

4.6. Nonparametric Statistical Tests (RQ2 & RQ3)

We compared high vs low groups for task performance and collaborate performance using (i) PERMANOVA to test for overall between-group differences in the multivariate action profile (Anderson, 2014), and (ii) Mann–Whitney U tests to test for action-specific pairwise differences (Mann and Whitney, 1947). PERMANOVA reports a permutation-based Pseudo-F statistic and p-value, making it well-suited for multivariate behavioral data that are typically non-normal, correlated across action dimensions, and not well-modeled by parametric MANOVA assumptions. Mann–Whitney U tests were used because individual action variables are often skewed/zero-inflated; we report U, raw p-values, and rank-based effect sizes (r) to quantify the magnitude and robustness of pairwise effects (Fritz et al., 2012).

Table 3
Socio-spatial learning behaviours identified from video recordings.

| Code | Socio-spatial learning behaviours description (primary and secondary ares) |
|-----------------------------|---|
| prim_Using_Computer | The students stay near the Bed 4 computer and use the computer to check/record information. |
| prim_Doc/Note_Interaction | The students interact with document/note at Bed 4. |
| prim_Using_Phone | The students pick up phones and chatting in a phone call. |
| prim_Medi/Equip_Interaction | The students conduct operations with medication or medical equipments near Bed 4. |
| prim_Patient_Interaction | The students interact with the patients at Bed 4 such as chatting or conduct some checks. |
| prim_Other | The students are moving, talking, or other unidentified behaviours at Bed 4. |
| sec_Using_Computer | The students stay near the Bed 1/2/3 computer and use the computer to check/record information. |
| sec_Doc/Note_Interaction | The students interact with document/note at Bed 1/2/3. |
| sec_Medi/Equip_Interaction | The students conduct operations with medication or medical equipments near Bed 1/2/3. |
| sec_Patient_Interaction | The students interact with the patients at Bed 1/2/3 such as chatting or conduct some checks. |
| sec_Other | The students are moving, talking, or other unidentified behaviours at Bed 1/2/3. |

4.7. Epistemic Network Analysis (RQ2 & RQ3)

Epistemic network analysis (ENA) (Shaffer et al., 2016) was conducted to examine the level of information captured by the socio-spatial learning behaviours generated from video data. This analysis was chosen as it has already been shown practical to uncover teamwork differences between low-performance and high-performance teams in clinical simulations (Yan et al., 2022b). The ENA Web Tool (version 1.7.0) (Marquart et al., 2018) was used to perform the analysis. For every second, a team was considered to perform an learning action that contained one or more of the seven learning behaviours (Table 2) or socio-spatial learning behaviours (Table 3). For example, if a team was engaged in *Using Computer*, *Doc/Note Interaction*, and *Medi/Equip Interaction* during one action, this action will be coded as (1,1,0,1,0,0,0) based on the order presented in Table 2, where 1 represents a team has demonstrated such learning behaviours and 0 represents the absence of such learning behaviours. A moving window size of six was used to capture the temporal connections between actions within a minute, specially the sequential relationships between a given action and the previous five actions. This value was chosen based on the learning design (Siebert-Evenstone et al., 2017) and because the patterns between the actions within one minute could indicate whether students were focusing on a particular task or shifting their attention across different tasks. Two comparison groups were formed based on teachers' assessment scores on task and collaboration performance. Based on teachers' inputs, teams with an average score within the range 4–7 were labelled as high-performing, and teams scoring 1–3 were labelled as low-performing. This labelling was done separately for task and collaboration performance. Comparison plots were computed for each scenario, and Mann-Whitney U tests were conducted to assess the statistical differences between low-performing and high-performing teams among the axes (Shaffer et al., 2016).

4.8. Dynamic Time Warping Analysis (RQ2 & RQ3)

Except for statistical tests and ENA analysis, we conducted a multivariate Dynamic Time Warping (DTW) analysis of behavioural action trajectories across simulation sessions (Sakoe and Chiba, 2003), representing each session as a continuous sequence of action-feature vectors. To enable comparability across action channels and across sessions, all features were globally standardized (z-scored) using a single scaler fit on the pooled observations from all sessions, so that subsequent contrasts can be interpreted in standardized units. Because session durations varied, each multivariate trajectory was temporally normalized by resampling to a common target length, which permits direct alignment,

Table 4
Inter-rater reliability at IoU ≥ 0.5

| Class | TP | FP | FN | P | R | F1 |
|------------------------|-----|----|----|-------|-------|-------|
| Overall | 399 | 31 | 26 | 0.928 | 0.939 | 0.933 |
| Using Computer | 50 | 1 | 2 | 0.980 | 0.962 | 0.971 |
| Doc/Note Interaction | 14 | 2 | 1 | 0.875 | 0.933 | 0.903 |
| Medi/Equip Interaction | 41 | 5 | 2 | 0.891 | 0.953 | 0.921 |
| Patient Interaction | 69 | 12 | 4 | 0.852 | 0.945 | 0.896 |
| Using Phone | 17 | 2 | 1 | 0.895 | 0.944 | 0.919 |
| Sitting | 44 | 0 | 0 | 1.000 | 1.000 | 1.000 |
| Other | 164 | 9 | 16 | 0.948 | 0.911 | 0.929 |

averaging, and visualization of action dynamics on a shared normalized timeline while retaining the full multivariate structure of the behavioural record.

To compare performance groups, we estimated separate group-level prototypical trajectories for high- versus low-performing sessions using DTW barycenter averaging (Petitjean et al., 2011) with a constrained warp path (Sakoe–Chiba band (Sakoe and Chiba, 2003)). DTW barycenters were selected because they accommodate non-linear differences in pacing and timing across sessions—an expected property of complex team behaviours—without forcing unrealistic pointwise alignment that could blur meaningful patterns. Group differences were quantified as action-wise contrasts between the high and low prototypes and summarized over the normalized timeline to yield a single standardized effect estimate per action (positive values indicate greater action intensity among high performers). To ensure that findings were not driven by an arbitrary temporal normalization, we performed a bootstrap sensitivity analysis (Tibshirani and Efron, 1993) across multiple candidate target lengths and selected an optimal length based on the stability of the resulting action-difference profile relative to a data-driven baseline (median session length). Stability was evaluated using complementary criteria—directional consistency (baseline-weighted sign agreement for effects above a minimum magnitude threshold) and rank-order agreement (Spearman correlation (Spearman, 2010))—and the final length was chosen using a conservative 1-standard-error rule (Hastie, 2009), prioritizing parsimonious normalization while maintaining robust, reproducible group-contrast patterns.

5. Results

5.1. RQ1 Result

Inter-rater reliability was assessed on randomly selected 100 images, which the two annotators labelled completely independently before seeing each other’s work. Within those images the raters produced 456 candidate activity instances. Using an IoU ≥ 0.50 only to decide whether two boxes referred to the same physical instance, they agreed on 399 objects and labels, disagreed on 57 (31 extra boxes, 26 missed boxes), and achieved an overall precision of 0.928, recall of 0.939, and F1 of 0.933. Per-class F1 values were uniformly high—perfect for *Sitting* (1.00) and ≥ 0.89 for every other category—showing that, in more than 9 out of 10 cases, both raters not only noticed the same object but also assigned it the same activity label. Minor differences in box tightness therefore have little practical impact on label consistency. After discussing and resolving the few disagreements observed in this pilot set, the annotators finalised the guidelines and proceeded to label the remainder of the dataset separately, confident that the protocol yields reliable, reproducible labels.

Figure 3 summarizes the optimization dynamics of the YOLOv11-based action detector over 70 epochs. All training losses decrease smoothly (train box/cls/df: 1.256/1.846/1.058 \rightarrow 0.732/0.340/0.892), while the corresponding validation losses exhibit a consistent downward trend and then saturate (val box/cls/df: 1.362/1.735/1.177 \rightarrow 0.999/0.595/0.952). This close coupling between training and validation trajectories indicates stable convergence and limited late-stage overfitting. Consistent with the loss behavior, the validation metrics increase rapidly in early epochs and plateau after approximately 40 epochs, reaching their best overall point at epoch 45 (Precision 0.886, Recall 0.883, mAP@0.5 0.933, mAP@0.5:0.95 0.691). The remaining gap between mAP@0.5 and mAP@0.5:0.95 suggests that residual errors are primarily attributable to tighter localization requirements (high-IoU regime) rather than coarse detection failures.

Table 5
Result of Model Running On Test Set

| Class | Images | Instances | Box(P | R | mAP50 | mAP50-95) |
|------------------------|--------|-----------|-------|-------|-------|-----------|
| all | 104 | 463 | 0.789 | 0.784 | 0.827 | 0.577 |
| Doc/Note Interaction | 24 | 28 | 0.563 | 0.429 | 0.542 | 0.436 |
| Medi/Equip Interaction | 35 | 51 | 0.756 | 0.73 | 0.8 | 0.519 |
| Other | 78 | 143 | 0.743 | 0.797 | 0.8 | 0.545 |
| Patient Interaction | 65 | 114 | 0.778 | 0.829 | 0.839 | 0.521 |
| Sitting | 47 | 47 | 0.991 | 0.979 | 0.993 | 0.683 |
| Using Computer | 43 | 64 | 0.693 | 0.844 | 0.824 | 0.624 |
| Using Phone | 16 | 16 | 1 | 0.881 | 0.995 | 0.709 |

The normalized confusion matrix in Figure 4 provides a class-level diagnostic and reveals strong diagonal dominance for most actions, indicating that the learned representation is largely class-consistent. The most reliable categories include Using Phone (1.00) and Sitting (0.97), while interaction-heavy categories show moderately lower diagonal mass (e.g., Doc/Note Interaction 0.77, Medi/Equip Interaction 0.82, Other 0.82, Patient Interaction 0.88, Using Computer 0.83). A recurring failure mode is confusion with background, which is particularly pronounced for semantically broad or visually ambiguous categories (e.g., Other \rightarrow background 0.31, Patient Interaction \rightarrow background 0.24, Using Computer \rightarrow background 0.21, Medi/Equip Interaction \rightarrow background 0.15). Beyond background leakage, misclassifications concentrate among semantically adjacent interaction classes (e.g., Patient Interaction \rightarrow Medi/Equip Interaction 0.09, Doc/Note Interaction \rightarrow Other 0.04), suggesting that the dominant residual errors arise from fine-grained inter-class ambiguity and contextual overlap rather than systematic collapse to a single label.

Figure 5 further supports the robustness of the detector across confidence thresholds. The aggregated precision–recall curve yields an overall $mAP@0.5 = 0.933$ on validation, showing that performance is not reliant on a single operating threshold but persists across a broad recall range. Per-class PR trends are consistent with the confusion-matrix diagnosis: visually distinctive or device-centric actions achieve near-ceiling separability (e.g., Using Phone 0.995, Sitting 0.991), whereas interaction-centric categories exhibit earlier precision degradation as recall approaches 1.0, especially Doc/Note Interaction (0.868). This pattern indicates that when the detector is pushed toward higher recall, false positives increase primarily in classes where the action cue is subtle and easily conflated with neighboring interactions or background-like frames.

Final generalization performance on the held-out test set is reported in Table 5. Overall, the model achieves Precision = 0.789, Recall = 0.784, $mAP@0.5 = 0.827$, and $mAP@0.5:0.95 = 0.577$ (Table 5, row “all”), demonstrating solid transfer from validation to test under a stricter, unseen distribution. Class-wise, Sitting and Using Phone remain strong ($mAP@0.5 = 0.993/0.995$, respectively), and Using Computer reaches competitive performance ($P = 0.693$, $R = 0.844$, $mAP@0.5 = 0.824$, $mAP@0.5:0.95 = 0.624$). In contrast, Doc/Note Interaction is the most challenging category ($P = 0.563$, $R = 0.429$, $mAP@0.5 = 0.542$, $mAP@0.5:0.95 = 0.436$). This degradation is consistent with the dataset characteristics: Doc/Note Interaction frequently occurs under partial occlusion and close-proximity multi-person overlap, and it is often spatially co-located with Using Computer (e.g., similar posture and shared workspace context). Such conditions reduce the separability of action-specific visual cues and increase both missed detections (lower recall) and confusion with neighboring interaction labels, which is also aligned with the inter-class ambiguity observed in Figure [Confusion Matrix] and the sharper precision drop at high recall in Figure [PR Curve]. Overall, these results indicate that the remaining bottleneck is not training instability but the fine-grained discrimination of overlapping, context-dependent interaction actions, especially in crowded or workstation-like scenes.

5.2. RQ2 Result

5.2.1. Statistical Tests Result

At the multivariate level, PERMANOVA provided no evidence of overall group differences in learning-action profiles for either grouping variable: task performance ($Pseudo-F = 1.093$, $p = 0.382$) and collaborate performance ($Pseudo-F = 1.201$, $p = 0.290$). Consistent with these global results, Mann–Whitney comparisons did not yield any learning-action category that remained significant after multiple-comparison adjustment. Although *Using phone* showed a nominal high–low difference for task performance ($U = 123.0$, $rawp = 0.027$, $r = 0.441$), this effect did not survive correction ($p_{adjusted} = 0.163$), and all other learning-action comparisons were non-significant after

adjustment. Overall, learning actions did not show a robust performance-linked pattern in either task or collaboration groupings.

5.2.2. ENA Result

The ENA projection plots show a clear separation between low- and high-performing teams along the first rotated dimension (MR1), indicating systematic differences in the learning behaviours that tended to co-occur. For task performance (Figure 6a), high-performing teams cluster more on the positive side of MR1 ($Mdn = 0.022, N = 40$), whereas low-performing teams cluster more on the negative side ($Mdn = -0.095, N = 11$), and this difference is statistically significant ($U = 106.000, p = 0.008, r = 0.518$). The behavioural structure associated with low task performance is dominated by connections involving *using phone* and *using computer*, suggesting teams may have invested more activity in technology-related actions that were less directly aligned with the core clinical tasks. In contrast, the high-performing pattern is characterised by tighter coupling among *Medi/Equip Interaction*, *Patient Interaction*, and *Doc/note Interaction*, reflecting greater focus on patient care actions and documentation that likely contributed to higher task scores.

A similar, though smaller, pattern is evident for collaboration performance (Figure 6b). High-collaboration teams again sit more on the positive side of MR1 ($Mdn = 0.028, N = 30$) compared with low-collaboration teams ($Mdn = -0.062, N = 21$), with a statistically significant difference ($U = 198.000, p = 0.025, r = 0.371$). The low-collaboration network is marked by dyadic links centred on *Using Phone* and *Using Computer*, whereas high-collaboration teams show stronger connections among clinically relevant behaviours (*Medi/Equip Interaction*, *Patient Interaction*, and *Doc/Note Interaction*). Overall, both figures suggest that higher task and teamwork outcomes are associated with behavioural coordination around patient care and medication/equipment work, rather than primarily around phone/computer use.

5.2.3. DTW Result

In the task performance grouped learning actions heatmap (DTW-barycenter prototypes; High $N = 40$, Low $N = 11$; time normalized to 0–1 with $L = 500$), the two performance groups exhibited distinct temporal organization of action intensity across the simulation. The most salient divergence was observed for *Using Phone*, where the Low group showed concentrated high-intensity episodes early-to-mid simulation (approximately the first half of the normalized timeline), whereas the High group showed comparatively sparse and lower-intensity phone activity. This pattern appears as sustained negative regions (blue) in the Difference (High - Low) panel for using phone, indicating that phone-related activity was systematically higher among low-performing sessions during these windows, rather than being driven by isolated spikes. In contrast, medications/equipment interaction and patient interaction in the High group displayed more sustained engagement later in the scenario (mid-to-late normalized time), producing predominantly positive difference regions (red) over extended segments of the trajectory; this suggests that higher-performing teams maintained more continuous task-relevant interaction with equipment/medications and the patient as the scenario progressed. Across the remaining channels, using computer and doc/note interaction exhibited more mixed, temporally localized contrasts (alternating small positive and negative bands), implying that group differences in documentation and computer use were less characterised by a single sustained shift and more by when these activities were deployed relative to the unfolding task.

In the collaborate performance grouped learning actions heatmap (DTW-barycenter prototypes; High $N = 30$, Low $N = 21$; normalized to $L = 300$), the most discriminative temporal signature between collaboration performance groups was concentrated in using phone. The Difference (High - Low) panel shows a pronounced, temporally localized negative band (blue) in the early-to-mid portion of the scenario (approximately 0.20–0.55 on the normalized time axis), indicating that low-collaboration sessions engaged in substantially more phone activity during this interval. This is consistent with the underlying barycenter data, where the low group exhibits sustained elevated phone intensity in that window while the high group remains largely near baseline. Because this contrast is sustained across a contiguous segment rather than appearing as isolated time-step spikes, it supports the interpretation of a systematic difference in communication/coordination behaviour (or off-task distraction) rather than a single anomalous episode.

Beyond phone use, group differences were more distributed and moderate in magnitude, but the directionality was interpretable and temporally coherent for several task-relevant actions. Across much of the mid-to-late scenario, the difference map indicates relatively higher *medi/equip* interaction and *patient interaction* in the high-collaboration group (predominantly positive regions), suggesting that teams with stronger collaboration performance allocate more behavioural “bandwidth” to direct patient care and equipment handling as the scenario unfolds. In contrast, using

computer and doc/note interaction display alternating small positive and negative regions across the timeline, implying that collaboration performance is not primarily characterized by overall increases/decreases in documentation or computer use, but rather by when these activities are scheduled relative to other actions. Finally, the other category shows broad time-varying contrasts; given its heterogeneous composition, interpretation should rely more on the stable, semantically specific effects (notably the early–mid excess in using phone among low collaborators and the comparatively greater late patient- and equipment-focused activity among high collaborators). For the Spatial Actions counterpart, the same action labels partitioned into primary versus secondary locations can be used to test whether these collaboration-linked differences (e.g., reduced phone use and increased patient/equipment engagement) are primarily executed in the primary working area or displaced into secondary areas, providing a location-sensitive explanation while preserving identical action semantics.

5.3. RQ3 Result

5.3.1. Statistical Tests Result

Spatial actions showed clear multivariate separation by performance. PERMANOVA indicated significant differences in the multivariate spatial-action profile for both task performance ($Pseudo-F = 2.933, p = 0.006$) and collaborate performance ($Pseudo-F = 2.446, p = 0.021$), implying that performance groups differed in how actions were distributed across locations (primary vs secondary) and action types.

Mann–Whitney tests localized this multivariate effect primarily to *prim_Patient Interaction*. For task performance, *prim_Patient Interaction* was significant and remained so after correction ($U = 363.0, rawp = 0.0011; p_{adjusted} = 0.0121; |r| = 0.650$), with higher means in the high-task group ($high_mean = 0.846 vs low_mean = 0.657$). For collaborate performance, *prim_Patient Interaction* was again significant after correction ($U = 492.0, rawp = 0.000730; p_{adjusted} = 0.00803; |r| = 0.562$), also showing higher means in the high-collaboration group ($high_mean = 0.878 vs low_mean = 0.701$). Other spatial comparisons did not consistently survive adjustment. Thus, the most robust and reproducible result is that higher-performing students exhibited greater patient interaction in the primary work area, aligning performance with increased engagement in the main workspace.

5.3.2. ENA Result

The ENA projection for task performance shows a clear separation between low- and high-performing teams along the first rotated dimension (MR1). High-performing teams are positioned more on the positive side of MR1 ($Mdn = 0.078, N = 40$), whereas low-performing teams are shifted toward the negative side ($Mdn = -0.257, N = 11$), and this difference is statistically significant with a large effect ($U = 359.000, p = 0.001, r = -0.632$). Consistent with this separation, the low-performing network is characterised by comparatively stronger connections among technology-focused and secondary behaviours (e.g., *prim_Using Phone*, *sec_Using Computer*, and *sec_Other*), suggesting attention was drawn toward less task-central activity patterns. In contrast, the high-performing network places greater emphasis on clinically relevant, primary-task connections—linking *prim_Patient Interaction*, *prim_Doc/Note Interaction*, and *prim_Medi/Equip Interaction*—indicating that teams with higher task scores coordinated their actions more around core patient-care work and documentation.

The ENA projection for collaboration performance shows a pronounced separation between low- and high-collaboration teams along MR1. High-collaboration teams are shifted to the positive side of MR1 ($Mdn = 0.095, N = 30$), whereas low-collaboration teams are centred on the negative side ($Mdn = -0.157, N = 21$), with a statistically significant difference and a large effect ($U = 505.000, p < 0.001, r = -0.603$). In the network structure, low-collaboration teams are characterised by stronger co-occurrences among technology-focused and secondary behaviours—particularly links involving *prim_Using Phone*, *sec_Using Computer*, and *sec_Other*—suggesting more coordination around peripheral or tool-use activities. By contrast, high-collaboration teams show relatively stronger connections among core clinical behaviours (e.g., *prim_Patient Interaction*, *prim_Medi/Equip Interaction*, and *prima_Doc/Note Interaction*), indicating that more effective teamwork was associated with coordinated engagement in patient care, medication/equipment use, and documentation.

5.3.3. DTW Result

In the task performance grouped spatial actions heatmap (DTW-barycenter prototypes; High $n = 40$, Low $n = 11$; normalized to $L = 200$), performance differences were expressed not only in what actions occurred, but where they were enacted (primary vs secondary locations). The most salient and temporally localized divergence again involved

prim_Using Phone: the Difference (High - Low) panel shows a strong negative band (blue) concentrated in the early-to-mid portion of the normalized timeline (roughly 0.20–0.50), indicating markedly higher phone activity in the primary work area among low-performing sessions. This spatially specific pattern supports the interpretation that, for low performers, phone use is not merely more frequent overall but is also disproportionately occurring in the most critical workspace, where it may directly compete with core patient-care behaviours. In contrast, high performers show comparatively reduced *prim_Using Phone* intensity during this same window, suggesting tighter behavioural focus in the primary area during key task phases.

Beyond phone use, the primary-location channels show a coherent shift toward patient- and equipment-facing work among high performers. The difference map indicates broadly positive regions (red) for *prim_Patient Interaction* and *prim_Medi/Equip Interaction* across much of the mid-to-late trajectory, consistent with sustained engagement in hands-on clinical activities in the primary workspace as the scenario progresses. Secondary-location channels exhibit smaller and more time-fragmented contrasts, implying that group separation is driven more by primary-area behavioural allocation than by a simple displacement of activity to secondary areas. Notably, several secondary actions (e.g., *sec_Using Computer* and *sec_Patient Interaction*) show mixed, alternating effects with limited temporal persistence, suggesting that secondary-space behaviour is more variable and less diagnostic of task performance than what occurs in the primary location. Overall, these spatially resolved prototypes indicate that high task performance is associated with minimizing disruptive behaviours (especially phone use) in the primary workspace while maintaining more sustained patient- and equipment-oriented activity there, whereas low performance is characterized by episodes of elevated primary-area phone use and less consistent primary-area clinical engagement.

In the collaborate performance grouped spatial actions heatmap, across the normalized collaboration timeline ($L = 700$), both performance groups exhibited a broadly similar spatial action profile: *prim_Doc/Note Interaction* remained relatively sustained across the session, while clinically oriented work in the primary area—especially *prim_Patient Interaction* and *prim_Medi/Equip Interaction*—became more prominent as the session progressed. Activity in the secondary area was more intermittent and diffuse, with *sec_Other* appearing throughout the sequence rather than being concentrated in a single segment, consistent with opportunistic movement to less-central areas. This overall similarity (predominantly comparable intensity bands in the High and Low heatmaps) suggests that group performance differences were not driven by a wholesale reorganization of the spatial workflow, but by more specific temporal reallocations of attention across action types and locations.

The Difference (High - Low) heatmap indicates that between-group contrasts were largely localized rather than global: most cells are near zero, but several time windows show coherent departures. Most notably, *prim_Using Phone* displays extended negative deviations (Low > High) in early-to-mid normalized time, implying greater reliance on phone use among lower-performing teams during periods when other primary-area tasks are concurrently active. In contrast, positive deviations (High > Low) are most evident for primary-area task engagement—particularly *prim_Patient Interaction* (and, to a lesser extent, *prim_Medi/Equip Interaction*) in mid-to-late normalized time—indicating that higher-performing teams spend relatively more time engaged in patient-facing and equipment-related actions in the primary workspace during the main body of the task. Differences involving the secondary area (e.g., *sec_Using Computer*, *sec_Patient Interaction*, *sec_Other*) appear smaller and more fragmented, suggesting that spatial performance differences are expressed primarily through how activity is allocated within the primary area (patient- and task-focused engagement vs. phone use), rather than through consistently increased time in secondary locations.

6. Discussion

7. Conclusion

References

- Ahuja, K., Kim, D., Xhakaj, F., Varga, V., Xie, A., Zhang, S., Townsend, J.E., Harrison, C., Ogan, A., Agarwal, Y., 2019. Edusense: Practical classroom sensing at scale. *PACM IMWUT* 3, 1–26.
- Akpen, C.N., Asaolu, S., Atobatele, S., Okagbue, H., Sampson, S., 2024. Impact of online learning on student's performance and engagement: a systematic review. *Discover Education* 3, 205.
- Alsharari, A.F., Salihu, D., Alshammari, F.F., 2025. Effectiveness of virtual clinical learning in nursing education: a systematic review. *BMC nursing* 24, 432.
- Alzoubi, D., Kelley, J., Baran, E., B. Gilbert, S., Karabulut Ilgu, A., Jiang, S., 2021. Teachactive feedback dashboard: Using automated classroom analytics to visualize pedagogical strategies at a glance, in: *Extended Abstracts of the 2021 CHI Conference on Human Factors in Computing Systems*, pp. 1–6.

- Anderson, M.J., 2014. Permutational multivariate analysis of variance (permanova). Wiley statsref: statistics reference online , 1–15.
- Blikstein, P., 2013. Multimodal learning analytics, in: LAK' 13, pp. 102–106.
- Bosch, N., Mills, C., Wammes, J.D., Smilek, D., 2018. Quantifying classroom instructor dynamics with computer vision, in: AIED, Springer. pp. 30–42.
- Bradski, G., 2000. The opencv library. Dr. Dobb's Journal: Software Tools for the Professional Programmer 25, 120–123.
- Buda, M., Maki, A., Mazurowski, M.A., 2018. A systematic study of the class imbalance problem in convolutional neural networks. Neural networks 106, 249–259.
- Burke, D., Crompton, H., Nickel, C., 2025. The use of extended reality (xr) in higher education: A systematic review. TechTrends , 1–14.
- Chen, A., Xiang, M., Zhou, J., Jia, J., Shang, J., Li, X., Gašević, D., Fan, Y., 2025. Unpacking help-seeking process through multimodal learning analytics: A comparative study of chatgpt vs human expert. Computers & Education 226, 105198.
- Chng, E., Seyam, M.R., Yao, W., Schneider, B., 2020. Using motion sensors to understand collaborative interactions in digital fabrication labs, in: AIED, Springer. pp. 118–128.
- Chua, Y., Cooray, S., Cortes, J.P.F., Denny, P., Dupuch, S., Garbett, D.L., Nassani, A., Cao, J., Qiao, H., Reis, A., et al., 2024. Striving for authentic and sustained technology use in the classroom: Lessons learned from a longitudinal evaluation of a sensor-based science education platform. International Journal of Human-Computer Interaction 40, 5073–5086.
- Echeverria, V., Yan, L., Zhao, L., Abel, S., Alfredo, R., Dix, S., Jaggard, H., Wotherspoon, R., Osborne, A., Buckingham Shum, S., et al., 2024. Teamslides: A multimodal teamwork analytics dashboard for teacher-guided reflection in a physical learning space, in: Proceedings of the 14th learning analytics and knowledge conference, pp. 112–122.
- Feng, S., Yan, L., Zhao, L., Maldonado, R.M., Gašević, D., 2024. Heterogenous network analytics of small group teamwork: Using multimodal data to uncover individual behavioral engagement strategies, in: Proceedings of the 14th learning analytics and knowledge conference, pp. 587–597.
- Fernandez-Nieto, G.M., Martinez-Maldonado, R., Kitto, K., Shum, S.B., 2021. Modelling spatial behaviours in clinical team simulations using epistemic network analysis: methodology and teacher evaluation, in: LAK21: 11th International Learning Analytics and Knowledge Conference, pp. 386–396.
- Fritz, C.O., Morris, P.E., Richler, J.J., 2012. Effect size estimates: current use, calculations, and interpretation. Journal of experimental psychology: General 141, 2.
- Hastie, T., 2009. The elements of statistical learning: data mining, inference, and prediction.
- Holm-Janias, V., Caro Miya Marshall, O., Li, Z., Bruun, J., Spikol, D., 2024. Design framework for multimodal learning analytics leveraging human observations, in: European Conference on Technology Enhanced Learning, Springer. pp. 106–112.
- Hsu, Y.C., Baldwin, S., Ching, Y.H., 2017. Learning through making and maker education. TechTrends 61, 589–594.
- Huang, S., Hou, Y., Liu, L., Yu, X., Shen, X., 2025. Real-time object detection meets dinov3. arXiv .
- Khanam, R., Hussain, M., 2024. Yolov11: An overview of the key architectural enhancements. arXiv preprint arXiv:2410.17725 .
- Kohnke, L., Fong, D., Chen, J., 2022. Using learner analytics to explore the potential contribution of multimodal formative assessment to academic success in higher education. Sage Open 12, 21582440221089957.
- Li, J., Liang, W., 2024. Effectiveness of virtual laboratory in engineering education: A meta-analysis. PloS one 19, e0316269.
- Li, T., Yan, L., Iqbal, S., Srivastava, N., Singh, S., Raković, M., Swiecki, Z., Tsai, Y.S., Gašević, D., Fan, Y., et al., 2025a. Analytics of self-regulated learning strategies and scaffolding: Associations with learning performance. Computers and Education: Artificial Intelligence , 100410.
- Li, X., Fan, Y., Li, T., Raković, M., Singh, S., van der Graaf, J., Lim, L., Moore, J., Molenaar, I., Bannert, M., et al., 2025b. The flora engine: Using analytics to measure and facilitate learners' own regulation activities. Journal of Learning Analytics 12, 391–413.
- Li, X., Li, T., Yan, L., Li, Y., Zhao, L., Raković, M., Molenaar, I., Gašević, D., Fan, Y., 2025c. Flora: An advanced ai-powered engine to facilitate hybrid human-ai regulated learning. arXiv preprint arXiv:2507.07362 .
- Li, X., Yan, L., Zhao, L., Martinez-Maldonado, R., Gasevic, D., 2023. Cvpe: A computer vision approach for scalable and privacy-preserving socio-spatial, multimodal learning analytics, in: LAK23: 13th International Learning Analytics and Knowledge Conference, pp. 175–185.
- Lim, F.V., O'Halloran, K.L., Podlasov, A., 2012. Spatial pedagogy: Mapping meanings in the use of classroom space. Cambridge journal of education 42, 235–251.
- Lv, W., Zhao, Y., Chang, Q., Huang, K., Wang, G., Liu, Y., 2024. Rt-detr2: Improved baseline with bag-of-freebies for real-time detection transformer. arXiv preprint arXiv:2407.17140 .
- Mallavarapu, A., Lyons, L., Uzzo, S., 2022. Exploring the utility of social-network-derived collaborative opportunity temperature readings for informing design and research of large-group immersive learning environments. Journal of Learning Analytics 9, 53–76.
- Mann, H.B., Whitney, D.R., 1947. On a test of whether one of two random variables is stochastically larger than the other. The annals of mathematical statistics , 50–60.
- Marquart, C.L., Hinojosa, C., Swiecki, Z., Eagan, B., Shaffer, D.W., 2018. Epistemic network analysis (version 1.7. 0)[software]. Available from app. epistemicnetwork. org .
- Martinez-Maldonado, R., Echeverria, V., Fernandez-Nieto, G., Yan, L., Zhao, L., Alfredo, R., Li, X., Dix, S., Jaggard, H., Wotherspoon, R., et al., 2023. Lessons learnt from a multimodal learning analytics deployment in-the-wild. ACM Transactions on Computer-Human Interaction 31, 1–41.
- Martinez-Maldonado, R., Echeverria, V., Santos, O.C., Santos, A.D.P.D., Yacef, K., 2018. Physical learning analytics: A multimodal perspective, in: LAK' 18, pp. 375–379.
- Martinez-Maldonado, R., Echeverria, V., Schulte, J., Shibani, A., Mangaroska, K., Shum, S.B., 2020. Moodoo: indoor positioning analytics for characterising classroom teaching, in: AIED, Springer. pp. 360–373.
- Nguyen, Q., Poquet, O., Brooks, C., Li, W., 2020. Exploring homophily in demographics and academic performance using spatial-temporal student networks, in: EDM'20, pp. 194–201.
- Ochoa, X., 2022. Multimodal learning analytics - rationale, process, examples, and direction, in: Lang, C., Siemens, G., Wise, A.F., Gašević, D., Mercer, A. (Eds.), The Handbook of Learning Analytics. 2 ed.. SoLAR, pp. 54–65. URL: <https://www.solaresearch.org/>

- publications/hla-22/hla22-chapter6/. section: 6.
- Ochoa, X., Lang, A.C., Siemens, G., 2017. Multimodal learning analytics. *The handbook of learning analytics* 1, 129–141.
- Papalazarou, N., Lefkos, I., Fachantidis, N., 2024. The effect of physical and virtual inquiry-based experiments on students' attitudes and learning. *Journal of Science Education and Technology* 33, 349–364.
- Paulsen, L., Lindsay, E., 2024. Learning analytics dashboards are increasingly becoming about learning and not just analytics—a systematic review. *Education and Information Technologies* 29, 14279–14308.
- Petitjean, F., Ketterlin, A., Gañcarski, P., 2011. A global averaging method for dynamic time warping, with applications to clustering. *Pattern recognition* 44, 678–693.
- Ramaswami, G., Susnjak, T., Mathrani, A., Umer, R., 2023. Use of predictive analytics within learning analytics dashboards: A review of case studies. *Technology, Knowledge and Learning* 28, 959–980.
- Riquelme, F., Noel, R., Cornide-Reyes, H., Geldes, G., Cechinel, C., Miranda, D., Villarroel, R., Munoz, R., 2020. Where are you? exploring micro-location in indoor learning environments. *IEEE Access* 8, 125776–125785.
- Rosa, C., Ferreira, J., 2023. The distant studio: a survey of design students' experience with distance educational formats. *International Journal of Technology and Design Education* 33, 2019–2043.
- Sakoe, H., Chiba, S., 2003. Dynamic programming algorithm optimization for spoken word recognition. *IEEE transactions on acoustics, speech, and signal processing* 26, 43–49.
- Saqib, N., Bose, A., George, D., Kamvar, S., 2018. Sensei: Sensing educational interaction. *IMWUT* 1, 1–27.
- Shaffer, D.W., Collier, W., Ruis, A.R., 2016. A tutorial on epistemic network analysis: Analyzing the structure of connections in cognitive, social, and interaction data. *Journal of Learning Analytics* 3, 9–45.
- Siebert-Evenstone, A.L., Irgens, G.A., Collier, W., Swiecki, Z., Ruis, A.R., Shaffer, D.W., 2017. In search of conversational grain size: Modeling semantic structure using moving stanza windows. *Journal of Learning Analytics* 4, 123–139.
- Spearman, C., 2010. The proof and measurement of association between two things. *International journal of epidemiology* 39, 1137–1150.
- Sümer, Ö., Goldberg, P., D'Mello, S., Gerjets, P., Trautwein, U., Kasneci, E., 2021. Multimodal engagement analysis from facial videos in the classroom. *IEEE Transactions on Affective Computing* 14, 1012–1027.
- Tibshirani, R.J., Efron, B., 1993. An introduction to the bootstrap. *Monographs on statistics and applied probability* 57, 1–436.
- Tkachenko, M., Malyuk, M., Holmanyuk, A., Liubimov, N., 2020-2025. Label Studio: Data labeling software. URL: <https://github.com/HumanSignal/label-studio>. open source software available from <https://github.com/HumanSignal/label-studio>.
- Torre, M.V., Tan, E., Hauff, C., 2020. edx log data analysis made easy: introducing elat: An open-source, privacy-aware and browser-based edx log data analysis tool, in: *Proceedings of the Tenth International Conference on Learning Analytics & Knowledge*, pp. 502–511.
- Tsai, T.H., Chang, C.H., Chen, S.W., 2016. Vision based indoor positioning for intelligent buildings, in: *2016 2nd International Conference on Intelligent Green Building and Smart Grid (IGBSG)*, IEEE. pp. 1–4.
- Yan, L., Martinez-Maldonado, R., Zhao, L., Dix, S., Jaggard, H., Wotherspoon, R., Li, X., Gašević, D., 2022a. The role of indoor positioning analytics in assessment of simulation-based learning. *British Educational Research Journal*, in press.
- Yan, L., Martinez-Maldonado, R., Zhao, L., Dix, S., Jaggard, H., Wotherspoon, R., Li, X., Gašević, D., 2022b. The role of indoor positioning analytics in assessment of simulation-based learning. *British Journal of Educational Technology*.
- Yang, Y., Wen, Z., Cao, J., Shen, J., Yin, H., Zhou, X., 2020. Epar: Early prediction of at-risk students with online and offline learning behaviors, in: *International Conference on Database Systems for Advanced Applications*, Springer. pp. 3–19.
- Zhang, X., Ding, Y., Huang, X., Li, W., Long, L., Ding, S., 2024. Smart classrooms: How sensors and ai are shaping educational paradigms. *Sensors (Basel, Switzerland)* 24, 5487.
- Zhang, Z., Cilloni, T., Walter, C., Fleming, C., 2021. Multi-scale, class-generic, privacy-preserving video. *Electronics* 10, 1172.
- Zhao, L., Echeverria, V., Tan, Y., Yan, L., Li, X., Alfredo, R., Dix, S., Jaggard, H., Wotherspoon, R., Osborne, A., et al., 2024a. Ordered networked analysis of multimodal data in healthcare simulations: Dissecting team communication tactics.
- Zhao, L., Swiecki, Z., Gasevic, D., Yan, L., Dix, S., Jaggard, H., Wotherspoon, R., Osborne, A., Li, X., Alfredo, R., et al., 2023a. Mets: Multimodal learning analytics of embodied teamwork learning, in: *LAK23: 13th International learning analytics and knowledge conference*, pp. 186–196.
- Zhao, L., Tan, Y., Gašević, D., Shaffer, D.W., Yan, L., Alfredo, R., Li, X., Martinez-Maldonado, R., 2023b. Analysing verbal communication in embodied team learning using multimodal data and ordered network analysis, in: *International Conference on Artificial Intelligence in Education*, Springer. pp. 242–254.
- Zhao, L., Yan, L., Gasevic, D., Dix, S., Jaggard, H., Wotherspoon, R., Alfredo, R., Li, X., Martinez-Maldonado, R., 2022. Modelling co-located team communication from voice detection and positioning data in healthcare simulation, in: *LAK22: 12th International Learning Analytics and Knowledge Conference*, pp. 370–380.
- Zhao, Y., Lv, W., Xu, S., Wei, J., Wang, G., Dang, Q., Liu, Y., Chen, J., 2024b. Detsr beat yolos on real-time object detection, in: *Proceedings of the IEEE/CVF conference on computer vision and pattern recognition*, pp. 16965–16974.

Scaffolding Enhance SRL

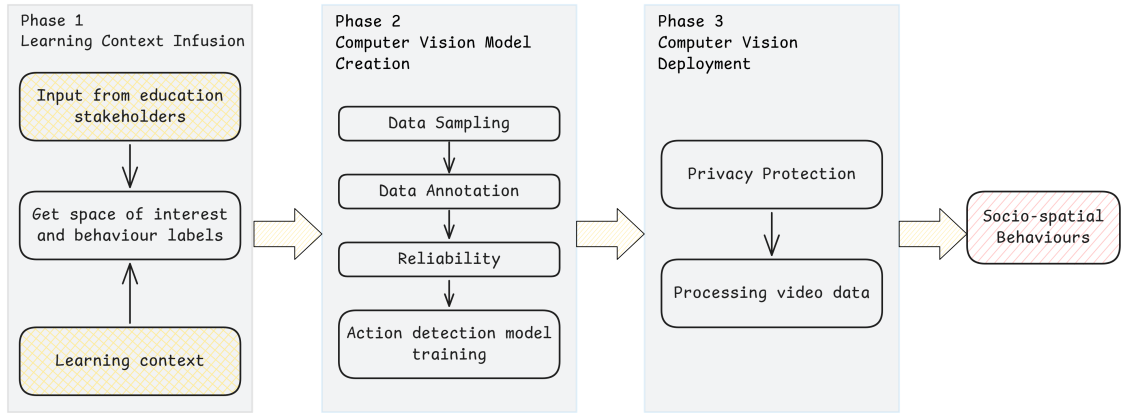


Figure 1: Computer vision approach for learning behaviours detection

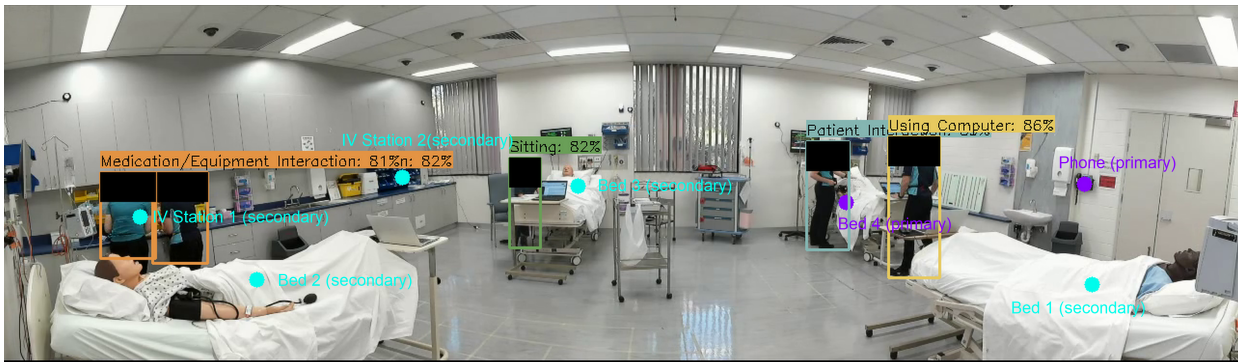


Figure 2: Teams of four students and a teacher playing the role of the patient in Bed 3's family member in the specialised classroom space. The points and labels represent the centre of different spaces of interest. The tracking boxes identify individuals and learning actions happened in the simulation classroom. The black area inside the tracking boxes protects individuals' facial identities.

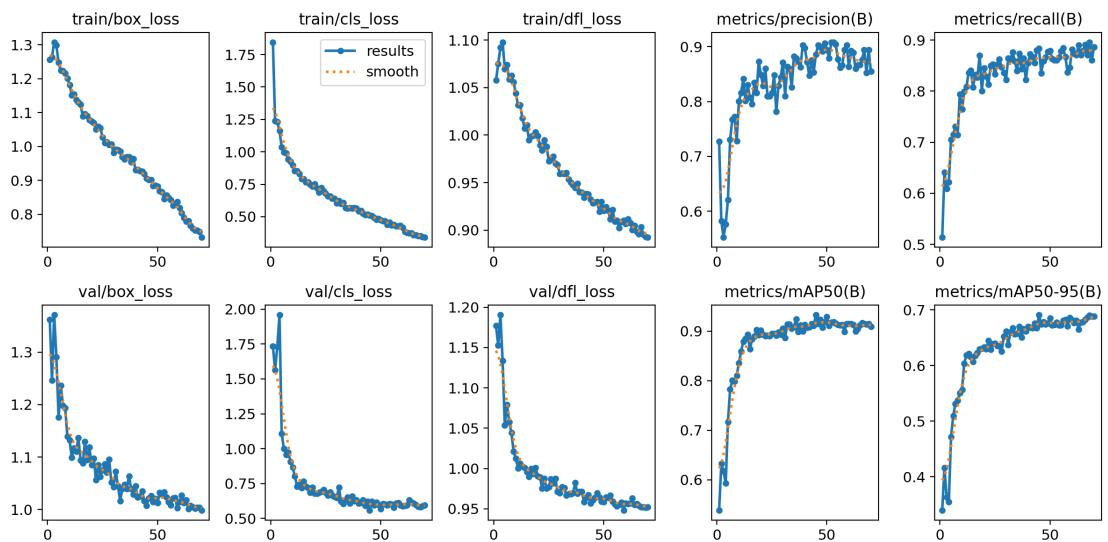


Figure 3: Model Training Results

Scaffolding Enhance SRL

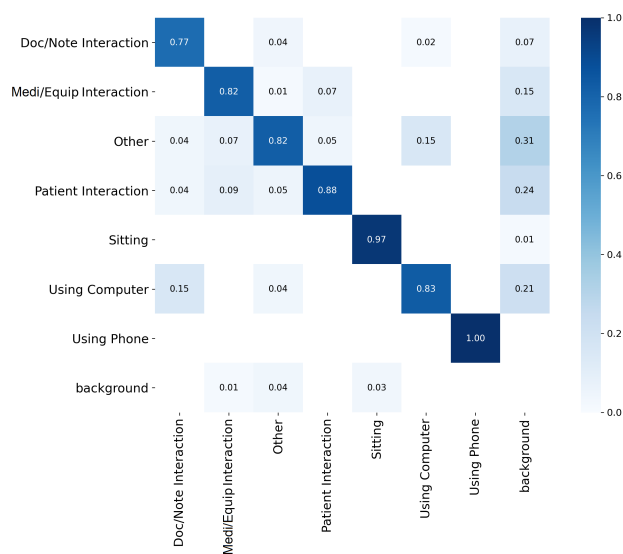


Figure 4: Confusion Matrix (Normalised)

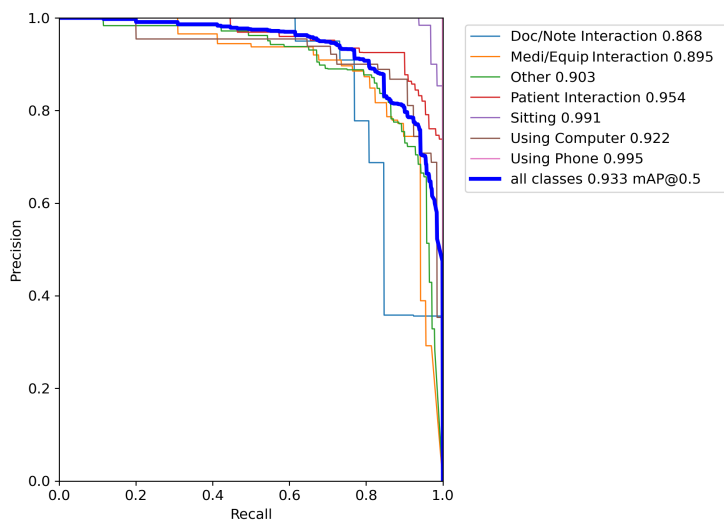


Figure 5: Precision Recall Curve

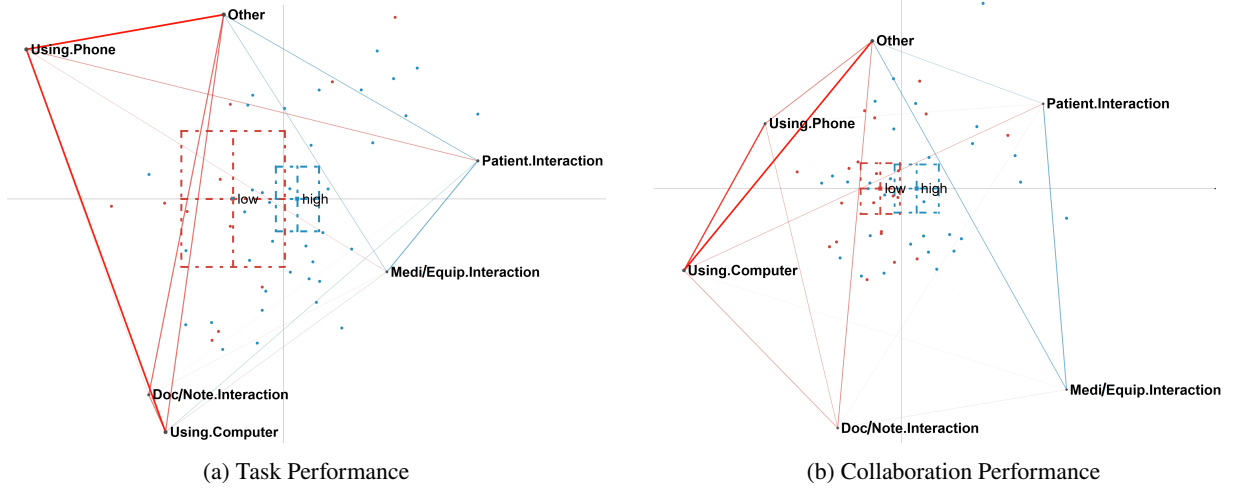


Figure 6: Learning Behaviours Analysis

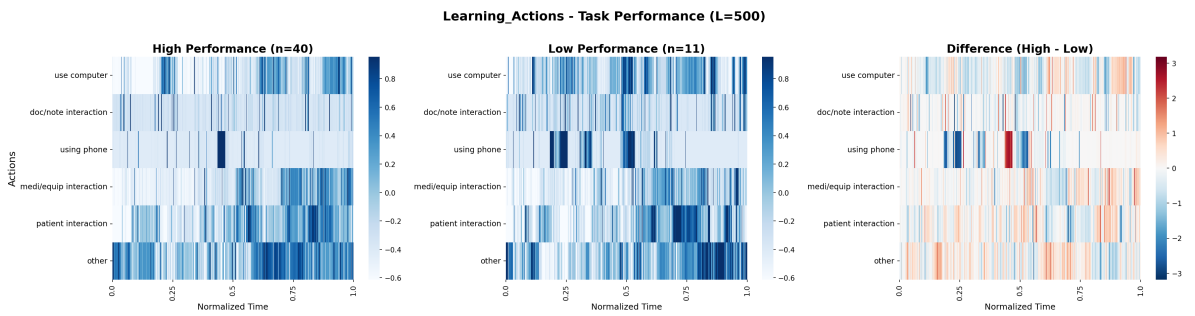


Figure 7: Temporal Organization of Learning Actions (Task Performance)

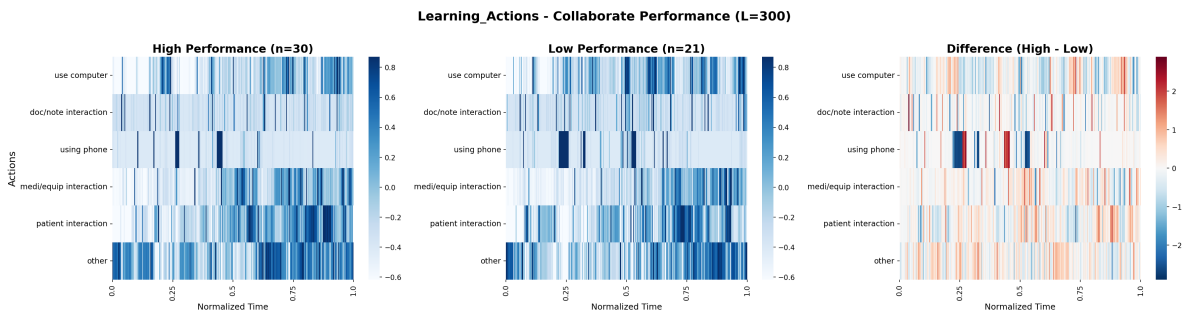


Figure 8: Temporal Organization of Learning Actions (Collaborative Performance)

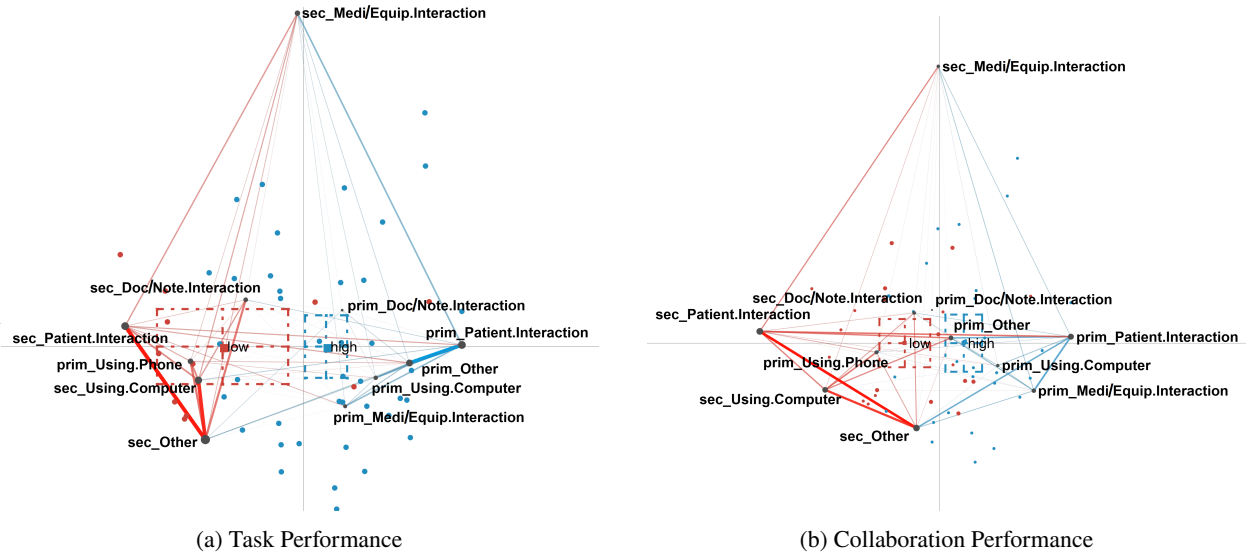


Figure 9: Spatial Learning Behaviours Analysis

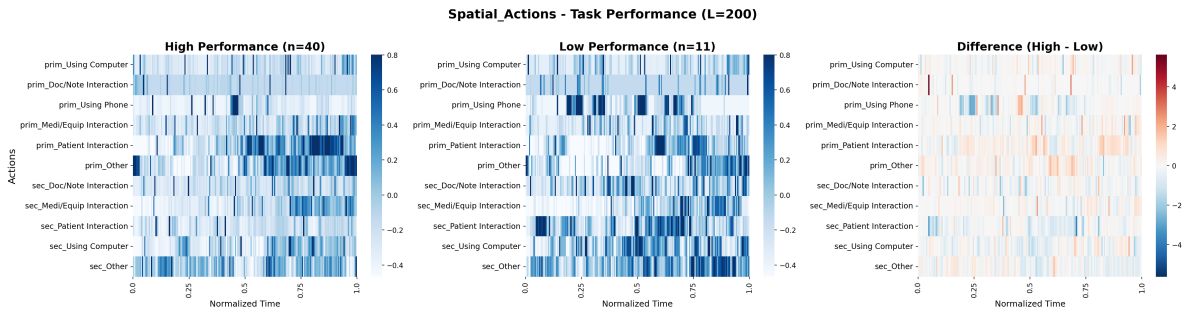


Figure 10: Temporal Organization of Spatial Actions (Task Performance)

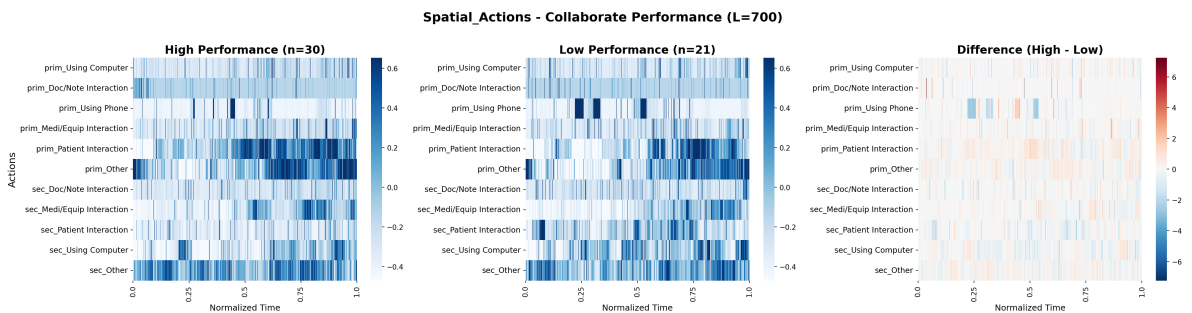


Figure 11: Temporal Organization of Spatial Actions (Collaborative Performance)